Available online at www.sciencedirect.com

ScienceDirect

Physics Procedia 10 (2010) 69–76

Physics Procedia

www.elsevier.com/locate/procedia

3rd International Symposium on Shape Memory Materials for Smart Systems

Creation of wear-resistant near-surface-layers with inhomogeneous structure on NiTi alloy by ion implantation technology

Z.Swiatek[a]*, N.Levintant-Zayonts[b], M.Michalec[c], T.Czeppe[a], M.Lipinski[a], O.Bonchyk[5], G.Savitskij[5]

[a]*Institute of Metallurgy and Materials Science PASc., 30-059 Krakow, 25 Reymonta str., Poland*
[b]*Institute of Fundamental Technological Research PASc., 02-106 Warsaw, 5B, Pawinskiego str., Poland*
[c]*Jagiellonian University, 30-069 Krakow, 3 Ingardena str., Poland*
[d]*Institute for Applied Problems of Mechanics and Mathematics NASU, 79 601 Lviv, 5 Naukova str., Ukraine*

Abstract

In the present study we report the changes in the modified near-surface layer on NiTi shape memory alloy, caused by ion implantation as well as their influence on the structure and mechanical properties of this material. Experimental results of an inhomogeneous structure and tribological properties of implanted NiTi are discussed in this paper.

Keywords: Shape memory NiTi alloy; ion implantation; DSC; X-ray diffractometry; TEM

1. Introduction

Among the many shape memory alloys (SMAs), NiTi alloys are the most popular, because they posess superior attributes in shape memory effect (SME) and pseudoelasticity (PE) [1,2]. Their particular and superior properties are caused by a reversible thermoelastic martensitic transformation. In general, NiTi alloys exhibit good biocompatibility and corrosion resistance, tolerance to severe environmental conditions, and thus are among the most important engineering materials. But, due to their poor tribological properties, the use of surface treatments to improve wear resistance is necessary. Additionally, the interest in shape memory alloys as biomaterials and their use in medical devices is increasing recently.

It is known that the problem of creating a protective surface coating on the shape memory alloy is the vital for potential applications of this material such as orthopedic devices, surgical tools, medical implants, endodontic

* Corresponding author. Tel.: +48-12-6374200; fax: +48-12-2952800.
E-mail address: nmswiate@imim-pan.krakow.pl.

1875-3892
doi:10.1016/j.phpro.2010.11.077

instruments and orthodontic wires in dentistry. In the case of NiTi, the problem of increasing of surface protective properties and, at the same time, preservation of functional properties of shape memory material is a subject of research and development [3]. In general, nitrogen implantation process may be one solution to enhance the mechanical properties of surface, corrosion, wear and fatigue resistance of shape memory alloy. Moreover, in the last year it is a new growth trend in materials science and surface engineering. Conventional ion implantation is a line-of-sight process in which ions are extracted from plasma, accelerated, and bombarded into a device. A systematic study of the effect of oxygen, carbon, zinc, zirconium and argon ions implantation on NiTi surface chemistry and its mechanical and shape memory properties for medical applications was conducted recently [4, 5]. Analysis of phase composition (GIXRD) revealed that the modified layers were the complex composites of implanted ions and the secondary phases of Ni-Ti. Many investigations explored the effect of ion implantation on the sequence of phase transformation, characteristic temperatures, structure changes in near-surface-layers of ion-implanted NiTi alloy and resulted in the alteration of the chemical composition of NiTi surfaces to a depth from a few hundred nanometers to 1 μm [6,7].

In the present study we report the changes in the modified near-surface layer on NiTi shape memory alloy, caused by ion implantation as well as their influence on the structure and mechanical properties of this material. Ion implantation is particularly adequate for the surface modification of NiTi alloy, because it is carried out at near-room temperature and therefore does not significantly change the bulk properties and microstructure of this alloy. Moreover, because the surface-modified layer is compositionally stepped, there is no clear interface between the surface-modified layer and the bulk material [5].

2. Experimental methods

In our investigation the equiatomic NiTi (Nitinol, Shape Memory Corporation, Japan) with martensitic type of structure has been used. NiTi samples (22×5.4×0.25 mm), were annealed for 30 min in vacuum at 300°C and then cooled in the furnace. The surface of the samples was cleaned using solution containing 10% $NClO_4$ and 90% acetic acid. Nitrogen ion implantation (at dose 1×10^{18} cm^{-2} and energy 55 keV) was carried out using typical semi-industrial implanter IMJON (Institute of Fundamental Technological Research PAS, Warsaw). It should be noted that in spite of the applied cooling, the additional ageing could take place during ion implantation process. The depth distributions of implanted and base atoms were estimated using SIMS technique.

Differential scanning calorimetry (DSC Q1000, TA Instruments) equipped with the liquid nitrogen cooling unit was used to characterize the sequence and the temperature ranges of the transformations for the initial, “as received” and surface-modified materials. Measurements were carried out in the helium gas atmosphere with a cooling/heating rates of 20°C /min.

For the X-ray diffractometry, the Philips diffractometer of the type X’Pert, in the Bragg-Brentano geometry was used to identify phase composition of the samples, both unimplanted and after implantation with nitrogen. CuKα radiation of the wavelength $\lambda = 0.154184$ nm was selected by the graphite monochromator. The scanning voltage of the X-ray tube was 40 kV, the current 25 mA, the exposure time 10 s and the angle, 2θ, was measured in the range 25^o to 95^o, while the scanning step was 0.02^o. The low temperature X-ray diffraction studies were carried out using the TTK Low-Temperature Camera (Anton Paar). The sample was heated from -50 up to +150°C in argon gas atmosphere. The measured angle 2θ was used from 35^o to 47^o. Lattice parameters were determined with use of the Philips X’Pert Plus software for all detected peaks. The effect of implantation irradiation on wear properties was investigated using an in-house built dry-sliding “ball-on-flat” wear tester (reciprocating motion, 6 mm diameter sapphire ball, stroke length 3 mm,).

Dry-sliding wear tests were done using load of 0.4N and 0.7N and several durations of dry-sliding test: 1h, 3h, 6h and 12h. Scanning profilometry method (HOMMEL-TESTER T8000 Nanoscan, Germany) was used to analyze the wear tracks, morphology of worn surface and to determine the wear loss of non-implanted and nitrogen implanted NiTi samples.

3. Results and discussion

Studies were started with DSC measurements. Samples weighted approximately 5 mg, in form of the very thin disc (0.25 mm) were analyzed with an empty aluminum pan as the reference. A temperature range from -50 to +150°C was scanned at a rate of 20°C/min during cooling and heating. The sequence started from the heating of the sample from low temperature up to 150°C and subsequent cooling back to -50°C. Results of two thermal cycles concerning the virgin and ion-implanted samples are shown in Fig. 1. As is shown, the alloy transforms to the martensite in two steps during cooling, showing two peaks in the all DSC curves representing cooling direction. As is well known for the equiatomic NiTi phase, the first peak correlates with the transformation from the austenite with the cubic B2 structure to the R-phase with a rhombohedral symmetry, being a rhombohedral distortion of the austenite. The second DSC peak represents transformation from the R-phase to the martensite with a monoclinic B19` structure. Similar two-step martensite phase transition from high temperature was reported for NiTi alloys after the thermo-mechanical treatment [8] or solution treatment and subsequent aging in case of the not equiatomic NiTi [9].

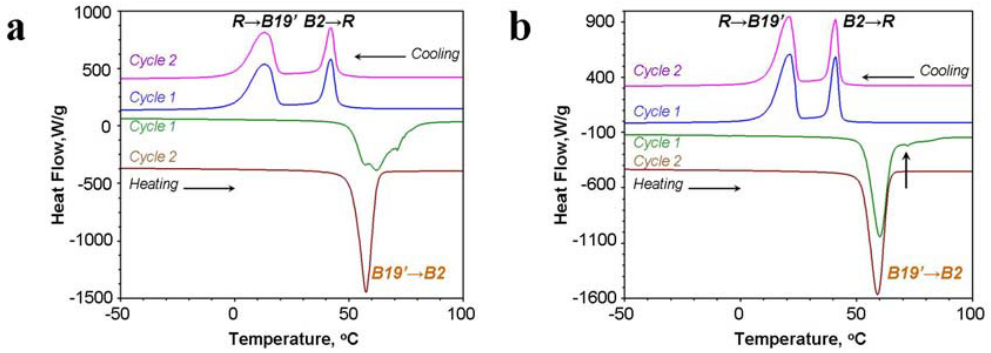

Fig.1. DSC curves of the virgin (a) and ion-implanted (b) alloys indicating a two-step phase transformation occurred during cooling.

Table 1. Transformation temperatures and enthalpy for the investigated non-implanted and implanted samples of NiTi alloy.

NiTi sample	cycle	Transformation	heating		cooling		
			A_s / °C	A_f / °C	R_s/M_s, /°C	R_f/M_f, /°C	Enthalpy / J/g
virgin	1	B19'→B2 R→B2	50.4	76.4	----	-----	23.5
		B2→R	----	----	45.1	37.8	24.5
		R→B19`	----	----	19.2	1.0	
	2	B19'→B2	51.6	62.3	----	----	24.7
		B2→R	----	----	45.1	37.8	24.7
		R→B19'	----	----	19.0	1.0	
ion-implanted	1	B19'→B2	53.2	65.6	-----	-----	26.1
		B2→R	-	-	43.3	37.2	27.0
		R→B19'	-	-	24.7	11.6	
	2	B19'→B2	52.5	64.0	----	----	27.2
		B2→R	----	----	43.3	37.4	27.0
		R→B19'	----	----	24.6	11.6	

More complicated effects were observed during heating cycles. During first heating (Fig.1a) the composed effect of reverse transformation was observed in place of one thermal effect representing B19'→B2 transformation as could be expected for equiatomic NiTi. The effect is composed from the tree parts suggesting overlapping of the B19'→B2, R →B2 and possibly deformation B19'→B2 transformations. The one-step transition B19'→B2 took place during second heating run (Fig.1a). In the case of the implanted sample in both heating runs one endothermic peak was observed (Fig 1b) resulting from the martensite to austenite transition. Additional, very small shoulder in the first heating run in Fig.1b, marked by the arrow may represent reverse transformation of the deformation martensite in the implanted layer. The transformation temperatures and transformation enthalpies of both investigated alloys are summarized in Table 1. The peaks in the heating direction corresponds to the martensite - austenite transformations started between 50.4°C and 53.2°C and finished between 62.3°C and 76.4 °C depending on the sample and cycle. Generally reverse transformation in the case of implanted sample started in the slightly higher temperature. The R_s temperature was stable for each sample, 45.1°C for not implanted and higher, 43.3°C for implanted, while the finishing temperatures of the B2→R transformation remains nearly the same, between 37.2-37.8°C. The M_s and M_f temperatures remains also stable in the cycles but slightly increased for the implanted sample in comparison with the not-implanted, with M_s=24.6°C and 19.0°C respectively. Also the difference in M_f temperatures was noticed meaning much broader temperature range of the R→ B19' transformation in case of the sample not implanted, 19°C in comparison wit 13.1°C. It should be noticed that enthalpy of transformations are larger for ion implanted samples. The results may suggest the influence of the internal stresses, structural or compositional inhomogeneity on the martensitic transformation in case of the implanted sample.

To verify above identifications, martensitic transformations in the NiTi alloys during heating and cooling were investigated in situ using the X-ray powder diffraction technique. The temperatures were reached by heating up and/or cooling down progressively after each measurement from 20°C. XRD results for the virgin NiTi alloy are shown in Figure 2.

From the analysis of the X-ray diffraction patterns it is evident that at 20°C on the first thermal cycle the virgin alloy exhibits two phases: the B19`-phase with a monoclinic structure and the R-phase, with a rhombohedral one. With increasing temperature, instead of the R-phase the B2-phase with a cubic structure appears. Simultaneously, no decreasing fraction of the B19`-phase, and an increasing fraction of the B2 was observed. From obtained results, it can be seen that, the B19`→B2- phase transformation finishes above temperature of 80°C. The X-ray diffraction obtained patterns for highest temperatures contain only reflections from the B2-phase and such phase composition do not change down to 150°C. Lowering the temperature up to about 42°C causes the appearance of the R-phase. In this temperature range the B2→R phase transformation starts and below the temperature of -25°C it finishes. Along with the decreasing the temperature, only the B19`-phase was observed. Such phase composition does not change down to 20°C and in this temperature only the B19`-phase exists in the start of second thermal cycle. The appearance of the R-phase in the virgin material in the temperature of 20°C on the first thermal cycle is related to thermal annealing at 300°C for 30 min before the investigations [10].

The X-ray diffraction patterns of the ion-implanted NiTi alloy against the temperature are shown in Fig. 3. From results obtained, it can be seen that the alloy in the temperature of 20°C exhibits three phases: the dominating B19`-phase and a small amount of the R2 and B2 phases. The appearance of austenite phase (crystalline, nano-crystalline and/or amorphous-like) may be related to structural changes in NiTi alloy during the ion implantation process and to high temperature of the target. The appearance of the R-phase, similar to results obtained for annealed materials, may be induced by high temperature of target. An increase of the temperature in material results in an increasing fraction of the B2 phase. From Fig. 3, it can be seen that the diffraction patterns of this B19`-phase do not change up to 65°C. Above this temperature an increasing fraction of the B2 phase and a distinct decreasing fraction of the B19` was observed. The B19`→B2 phase transformation finishes above temperature of 80°C. The X-ray diffraction patterns obtained for highest temperatures (from 80°C to 150°C) contain only reflections from the B2-phase. Lowering the temperature up to about 41°C, beside still existing the B2 phase, the R-phase appears. From results obtained, it can be seen that, the R→B19`-phase transformation starts from the temperature of 25°C and finishes about -25°C. Along with the decreasing the temperature, beside the dominating B19`-phase, a small amount of the B2-phase was detected. Such phase composition was also observed for material at 20°C on the start and finish of second thermal cycle. The broad structure of this diffraction peak may testify that still some amount of the amorphised and/or nano-crystalline B2 phase is present in the alloy.

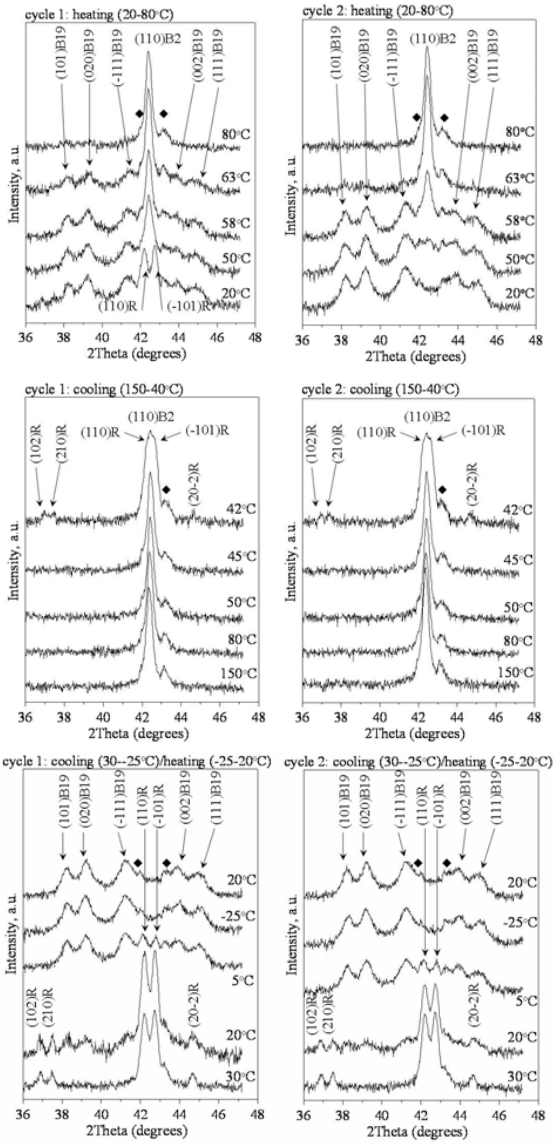

Fig. 2. The recorded X-ray diffraction patterns versus the temperature of NiTi alloy after thermal annealing at 300 °C for 30 min before an ion implantation.

In the process of ion implantation of nitrogen at fluence 10^{18}cm^{-2} and 50keV energy, the well-defined double-layer structure with different microstructure as well as different phase and chemical composition was formed (Fig. 4). During an ion implantation, collisions between incident ions and NiTi-target atoms lead to the formation of near-surface amorphized layer (A-layer, Fig. 4a) and extended defects in the crystalline structure of bulk material (D-layer and Bulk on Fig. 4a). The transition zone of a damaged region is wide and its composition changes gradually from totally amorphized Ti-rich material (heavily damaged and nanocrystalline) to Ni-rich crystalline (A1 and A2 regions in A-layer on Fig. 4b). Amorphous-like layer contains some amount of crystalline inclusions within its bulk,

mainly near a bottom boundary of transition zone. From 80 to 160 nm depth the material has defected crystalline microstructure. In deeper layers, the unaffected grain structure can be seen.

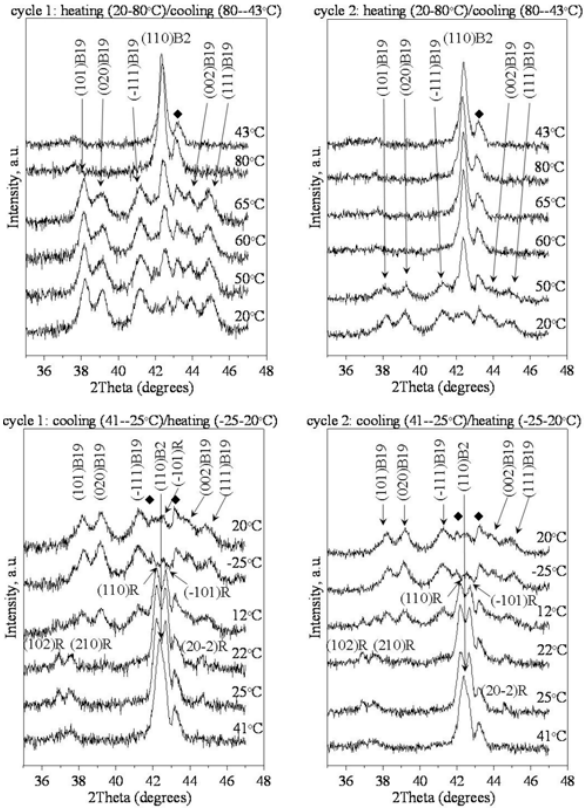

Fig. 3. The recorded X-ray diffraction patterns versus the temperature of ion-implanted NiTi alloy at fluence 10^{18}cm^{-2} and energy 50keV.

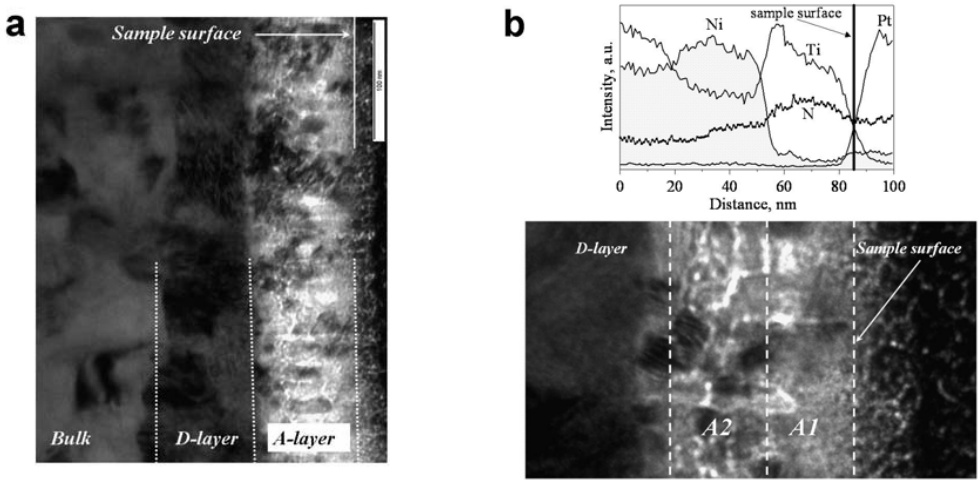

Fig. 4. Bright-field image of the ion-implanted NiTi alloy demonstrating the structural and chemical composition changes in near-surface layers.

In order to determine the wear loss surfaces, the wear tracks formed on the implanted and non-implanted sample surface were analyzed by means of the Hommel Map Expert 4.1 software. It enables to estimate the volume of grooves produced in the wear process. Fig.5 shows 3-D maps of worn surface for the non-implanted (a) and implanted (b) surface NiTi. It can be seen that wear volume for implanted surface is lower than in the case of the non-implanted material. As shown in Fig.5 surface-implanted sample exhibits a better wear resistance than the base material. Fig.6 (a, b) shows the wear volume as a function of the dry-sliding time.

The sliding wear resistance has been effectively improved by the surface treatment. This increased resistance was attributed to the formation of a thin modified layer. In our case, we have seen large quantities of composition-impurities at the implanted surface, especially carbon and oxygen which was the dominant element up to approximately ~10μm - 25μm [11]. Considering the observed concentrations of Ti, O, C and N, - it is possible, that such oxinitrides and carbides moderate the wear processes and an improvement in the wear resistance takes place. Significant improvements of wear resistance of ion-implanted NiTi-alloy owing to creation in near surface region the double-layer structure with different microstructure, phase and chemical composition were observed.

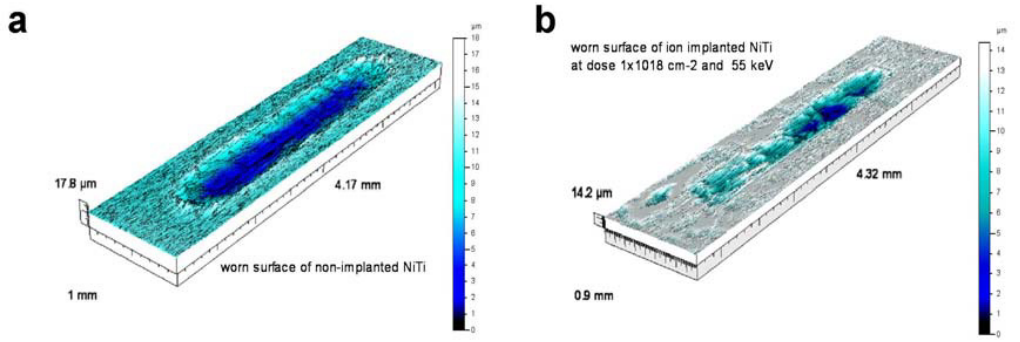

Fig. 5. 3D-view of worn NiTi surface maps (load 0.7 N and time of dry-sliding process 12h) and morphology of wear tracks: (a)-before and (b)-after nitrogen implantation at 1×10^{18} cm^{-2} ion dose and energy 55 keV.

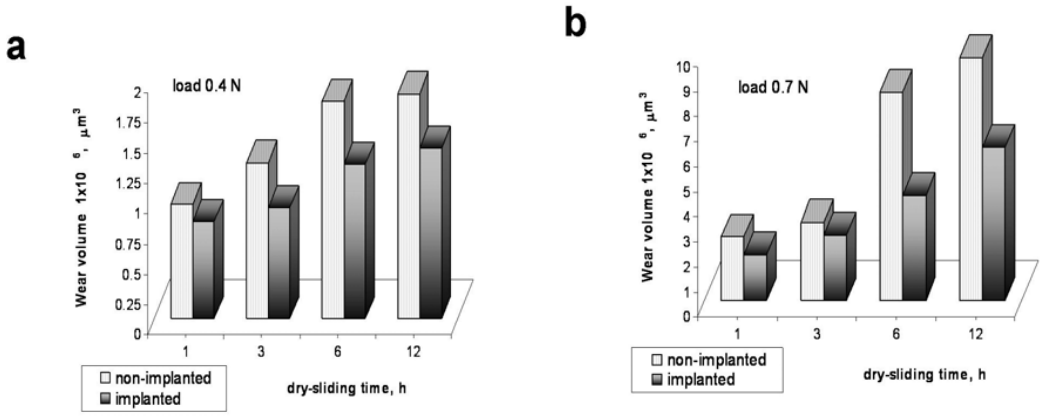

Fig. 6. Volume of wear loss for nitrogen implanted ($1\times10^{18}cm^{-2}$, 55 keV) and non-implanted NiTi samples at several times of dry-sliding test: (a) load 0.4 N; (b) load 0.7 N.

We assume that after ion implantation the surface-modified layer is compositionally stepped, there is no clear interface between the surface-modified layer and the bulk material. This is a critical point (because the surface layer must be suitable to undergo large reversible strain when the bulk material transforms) and require the subsequent investigation. Further experiments in order to clarify the nature of inhomogeneous structure created by ion irradiation and its influence on the mechanical properties of NiTi alloy will be carried out. The result may be applied to the precise verification of shape memory effect for future MEMS (micro-electro mechanical systems) devices, since it is well known that the lattice defect density in modified surface affects physical and mechanical properties, i.e. shape recovery temperature, shape recovery strains, wear and fatigue life and etc.

4. Conclusions

In the present study we presented our research of inhomogeneous near-surface layers in ion implanted (at dose 1×10^{18}cm^{-2} and energy 55 keV) equiatomic NiTi shape memory alloy and characterization using the electron microscopy and X-ray study of structural evolution, additionally the wear test of mechanical properties in implanted NiTi alloy.

To characterize the transformation sequence and transformation temperatures DSC measurements were carried out on an unimplanted as well as an implanted material. Both the unimplanted and ion-implanted NiTi alloys transform in two steps (B2→R→B19') in the cooling direction and the one-step transition (B19'→B2) in the heating process. To verify identification of martensitic transformations in the NiTi alloys during heating and cooling, the X-ray structural investigations were performed.

The TEM structural characterization reveals the existence of the well-defined double-layer structure with different microstructure as well as different phase and chemical composition in near surface region of ion-implanted NiTi-alloy. From the surface to a depth of 80 nm the sample has an amorphized structure in the form of two sublayers: the first is a Ti- and N-rich nano-crystalline and/or amorphous-like and the second - Ni-rich crystalline). From 80 to 160 nm depth, the material has a defect Ti-rich crystalline microstructure and deeper - unaffected grain structure of parent material.

Dry-sliding wear test reveals the increase of wear resistance in nitrogen ion implanted NiTi alloy owing to formation of complexity, inhomogeneous structure and phase conditions in near-surface region after ion irradiation.

References

1. Humbeeck J. Scripta Materialia 50 (2004) 179.
2. Chrobak D, Morawiec H. Scripta materialia 44 (2001) 725.
3. Pelletier H, Muller D, Mille P, Grob J Surf.& Coat. Techn. 158 (2002) 309.
4. Shabalovskaya S, Andregg J, J.Van Humbeeck. Acta Biomaterialia 4 (2008) 447.
5. Tan L, Crone W.C, Acta Materialia 50 (2002) 4449.
6. Mandl S. Surface and Coatings Technology 201 (2007) 6833.
7. Jinlong Li, Migren Sun, Xinxin Ma, Guangze Tang. Wear 261 (2006) 1247.
8. H. Morawiec, D. Stroz, T. Goryczka, D. Chrobak, Scr. Mater. 35 (1996) 485.
9. M. Nishida, T. Honma, Scr. Metall. 18 (1984) 1293.
10. Su-Young Cha and Se-Young Jeong, Jeung Hun Park, Sang Eon Park, Jong Kweon Park, Chae Ryong Cho, Journal of the Korean Physical Society 49 (2006) S580.
11. N. Levintant-Zayonts, S. Kucharski, Vacuum 83 (2009) S220.